
RUSH: ROBUST CONTRASTIVE LEARNING VIA RANDOMIZED SMOOTHING

Yijiang Pang, Boyang Liu, Jiayu Zhou
 Department of Computer Science and Engineering
 Michigan State University, East Lansing, MI 48823, USA
 {pangyiji, liuboya2, jiayuz}@msu.edu

ABSTRACT

Recently, adversarial training has been incorporated in self-supervised contrastive pre-training to augment label efficiency with exciting adversarial robustness. However, the robustness came at a cost of expensive adversarial training. In this paper, we show a surprising fact that contrastive pre-training has an interesting yet implicit connection with robustness, and such natural robustness in the pre-trained representation enables us to design a powerful robust algorithm against adversarial attacks, RUSH, that combines the standard contrastive pre-training and randomized smoothing. It boosts both standard accuracy and robust accuracy, and significantly reduces training costs as compared with adversarial training. We use extensive empirical studies to show that the proposed RUSH outperforms robust classifiers from adversarial training, by a significant margin on common benchmarks (CIFAR-10, CIFAR-100, and STL-10) under first-order attacks. In particular, under ℓ_∞ -norm perturbations of size 8/255 PGD attack on CIFAR-10, our model using ResNet-18 as backbone reached 77.8% robust accuracy and 87.9% standard accuracy. Our work has an improvement of over 15% in robust accuracy and a slight improvement in standard accuracy, compared to the state-of-the-arts.

Keywords Robustness · Randomized Smoothing · Contrastive Learning

1 Introduction

Adversarial attacks have imposed a significant challenge to inference robustness of machine learning models. For example, an image classifier that achieves high accuracy for normal testing data could be easily fooled by a perturbed image from adversarial attacks, and the perturbed images usually have very subtle differences from normal images [1, 2]. To tackle this challenge, many defense mechanisms are proposed to achieve adversarial robustness [3, 4, 5, 6]. The defense algorithms can be categorized into empirical defense and certified defense, where the latter provides provable robust guarantees (i.e. there exist no adversarial samples given bounded perturbation). One popular empirical defense is adversarial training (AT), which augments training data with adversarial examples. AT is usually achieved by alternative min-max optimization [1, 7]. However, failed adversarial examples from unstable attacks may break the defense, as a result of numerical instability, randomness, and vanishing/exploding gradients [8].

On the other hand, certified defenses provide provable robustness that the predictions of classifier remain constant within certain neighborhoods. One class of approaches reach certified robustness through robust training, which are guaranteed to detect all adversarial examples around a data point in a norm-bounded range by constructing an upper bound on the worst-case loss through convex relaxations [9, 10]. Due to large computational costs, those methods are mostly restricted to applications of small-scale data. Randomized smoothing provides certified defenses for large datasets. It smooths a classifier by applying the convolution between Gaussian noise and the classifier, and is certifiably robust to adversarial perturbations under the ℓ_2 norm [11, 5]. Although certificated defense can provide us theoretical guarantees against the adversarial attack, compared with the empirical defense such as adversarial training, the empirical performance of certificated defense is usually worse than empirical defenses.

Introducing robustness in Self-Supervised Learning (SSL) recently has attracted significant efforts from the community [12, 13, 14], as recent years witnessed its huge success in many applications that dramatically improves

generalization performance by leveraging unlabeled data for downstream tasks. A typical SSL treatment includes a self-supervised contrastive pre-training stage, followed by a supervised fine-tuning stage that tailors the pre-trained model to supervisions [15, 16, 17, 18]. Unfortunately, recent studies showed that SSL does not spare from robustness issues [12, 13, 14]. Attempts of integrating adversarial training in SSL have demonstrated improving robustness by paying the price of expensive computation costs that can be forbidden in many resource-limited data mining applications [19, 6].

As such, in this paper, we ask the following intriguing and important question: *is adversarial training necessary to achieve robustness in contrastive pre-training?* By studying the similarity between Lipschitz continuity and optimization objective of contrastive learning (c.f. Section 4.1), we reveal the *natural robustness* introduced by contrastive learning. With such robustness, we propose an embarrassingly simple framework to deliver powerful robustness by combining contrastive learning and randomized smoothing. We demonstrate that the model trained with the proposed approach, which follows the SimCLR training procedures, shows significant robustness to Projected Gradient Decent (PGD) attack [4] and AutoAttack (AA) [20] on CIFAR-10, CIFAR-100, and STL10, achieving state-of-art accuracy for clean data and perturbed data [21, 22]. Specifically, using ResNet-18 as backbone and general training hyper-parameters, pure SimCLR reached 92.6% accuracy in clean data on CIFAR-10. Our method reached 87.9% accuracy in clean data and 77.8% accuracy in PGD attacked data. Notably, our approach hardly introduces extra computational overhead in the both pre-training and fine-tuning stages compared with SimCLR.

Our contributions. Our paper has the following contributions. Firstly, we discuss the potential connection between Lipschitz continuity and contrastive pre-training, which leads to the discovery of hidden natural robustness induced by contrastive learning. Secondly, our proposed approach, which strategically combines the natural robustness with randomized smoothing, has shown significant robustness against first-order-based attacks with a very limited sacrifice of the standard accuracy. Finally, we conducted extensive empirical studies to evaluate the proposed algorithm, which delivers comparable results against state-of-the-arts while enjoys much smaller training costs.

2 Related Work

Adversarial Training. Existing literature studied the adversarial robustness of neural networks [23, 24, 25, 26]. Adversarial training (AT) is one of the most powerful methods against adversarial attacks [4], which injects adversarial examples in the original training set. AT is usually associated with huge computational overhead, leading to efforts on data-efficient and computation-efficient variants to mitigate the cost of the generating of adversarial examples [27, 28, 29]. However, these approaches still demand considerable additional computational costs for constructing and augmenting adversarial examples as compared to the standard training.

Adversarial Training in Self-supervised Learning. Recently, adversarial examples were shown to improve the robustness of self-supervised learning [12]. Continued efforts developed a variety of approaches to introduce adversarial training in the context of self-supervised learning [13, 19, 14]. A prominent example is SimCLR, a popular and simple contrastive learning framework with exceptional performance [17]. Injecting adversarial samples to the pre-training stage of SimCLR is shown to successfully induce model robustness [6]. Alternatively, robustness can be achieved by a training process that maximizes the similarity between a random augmentation of a data sample and its instance-wise adversarial perturbation [30]. Most existing robust approaches in contrastive learning rely on adversarial training, which is associated with significant computational overhead and decreased standard accuracy, and often provides no provable guarantees.

Certified Defenses. In contrast to empirical approaches for robustness such as adversarial training, certified defense guarantees provable robustness to a specific class of adversarial perturbation [31, 32, 33, 34, 9, 35, 10]. Many existing approaches admit efficiency issues and are hard to scale to large datasets [5, 11].

Randomized smoothing, a kind of certified defenses, was developed following the idea of augmenting the dataset by sampling some data points centered at the original data examples in the input space to against adversarial perturbation [36, 37], but no guarantees have been proved in these works. Following works largely expanded the generalization of randomized smoothing and proved its robustness guarantee against ℓ_p -bounded adversaries [11, 38, 39, 40]. A recent work comprehensively studied the interaction between two important factors of random smoothing: the choice of smoothing distribution and the perturbation norm [41]. Combining adversarial training with randomized smoothing classifiers is recently shown to substantially boost certified robustness [5], and it suffers the aforementioned issues due to its usage of adversarial training. Besides, the accuracy trade-off has also been observed in randomized smoothing that adversarially trained networks with higher robust accuracy tend to have lower standard accuracy [42, 11].

3 Notations and Preliminaries

In this section, we introduce notations and revisit preliminaries, including contrastive learning, randomized smoothing, and adversarially perturbed data. We use $(\mathbf{x}_i, \mathbf{y}_i)$ to denote one single labeled data point or an observation, and the training set $\mathcal{D} = \{\mathbf{x}_i, \mathbf{y}_i\}_{i=1}^k$.

Contrastive Learning is a technique that uses unlabeled data to learn feature representations by constructing supervisions of similarity/dissimilar pairs from data. SimCLR is a widely-adopted contrastive learning framework [17] due to its high performance and simplicity. We will use SimCLR as our backbone of contrastive learning for discussion in this paper.

Formally, SimCLR has two stages: self-supervised pre-training and supervised fine-tuning. During the pre-training stage, it leverages a set of pre-defined data transformations \mathcal{T} , samples two transformations $t_1, t_2 \sim \mathcal{T}$, and uses them to transform a given data point \mathbf{x} into two views $t_1(\mathbf{x}), t_2(\mathbf{x})$. It then uses a multi-view contrastive learning loss \mathcal{L}_{pre} to learn a feature extractor and projector $g_{\theta_p} \circ f_{\theta}$, where the model equipping with projector $g(\cdot)$, parameterized by θ_p , on top of the feature extractor $f(\cdot)$, parameterized by θ . The loss maximizes the cosine similarity of the projected data representations of different views of the same image and minimizes the cosine similarity of the projected data representations generated by different images. In the fine-tuning stage, it uses the labeled training data in \mathcal{D} to learn a classifier $\phi(\cdot)$, parameterized by θ_c , with representations from the feature extractor $f(\cdot)$. The objectives are given by:

$$\begin{aligned} \text{PRE-TRAIN: } & \min_{\theta, \theta_p} \mathbb{E}_{t_1, t_2 \sim \mathcal{T}, \mathbf{x} \in \mathcal{D}} \mathcal{L}_{pre}(g_{\theta_p} \circ f_{\theta}([t_1(\mathbf{x}), t_2(\mathbf{x})])); \\ \text{FINE-TUNE: } & \min_{\theta_c} \mathbb{E}_{\mathbf{x}, \mathbf{y} \in \mathcal{D}} \mathcal{L}_{CE}(\phi_{\theta_c} \circ f_{\theta}(\mathbf{x}), \mathbf{y}). \end{aligned}$$

Randomized Smoothing aims to construct a smooth classifier G from a base classifier $F : \mathcal{X} \in \mathbb{R}^d \rightarrow \mathcal{Y} \in \mathbb{R}$ that maps an instance space \mathcal{X} to an output space \mathcal{Y} . The smoothed classifier G responds to a query \mathbf{x} with the class that the base classifier F is most likely to return when \mathbf{x} is perturbed by isotropic Gaussian noise [11, 5]:

$$G(\mathbf{x}) = (F * \mathcal{N}_d(0, \sigma^2))(x) = \mathbb{E}_{\delta \sim \mathcal{N}_d(0, \sigma^2)} [F(\mathbf{x} + \delta)], \quad (1)$$

where σ denotes noise level to trade-off between robustness and accuracy.

There are several approaches to train a smoothed classifier [11, 5, 43]. In this paper, we use the following representative method, one-time-noise-based augmentation, to train our classifier:

$$\mathcal{L}(\mathbf{x}, \mathbf{y}) = -\log F(\mathbf{x} + \delta)_{\mathbf{y}}, \quad (2)$$

where δ is sampled from smoothing distribution. The choice of smoothing distribution including its noise scale is key to empirical success of random smoothing [41]. We denote the randomized smoothing operator to data \mathbf{x} as $\mathcal{Q} : \mathbb{R}^d \rightarrow \mathbb{R}^d$:

$$\mathcal{Q}(\mathbf{x}) = \mathbf{x} + \delta, \quad (3)$$

where $\delta \in \mathbb{R}^d \sim \Omega_d$ is a vector sampled from a certain smoothing distribution Ω_d . Common choices of smoothing distributions include uniform distribution $\delta \sim U_d(-\mu, \mu)$ and Gaussian distribution $\delta \sim \mathcal{N}_d(0, \sigma^2)$. A comprehensive study of various smoothing distributions is provided in [41].

During the inference, randomized smoothing uses Monte-Carlo sampling to estimate the expectation in equation 1. Similarly, we use a voting strategy, denoted by $\mathcal{V}_m(F(\mathbf{x}))$, to estimate the expected prediction \hat{y} for an input \mathbf{x} , from outputs generated by m times randomly smoothed \mathbf{x} :

$$\hat{y} = \text{VOTING} (F(\mathcal{Q}_i(\mathbf{x}))) = \text{VOTING} (F(\mathbf{x} + \delta_i)) \equiv \mathcal{V}_m(F(\mathbf{x})), \quad (4)$$

where m is a hyper-parameter. A relatively larger m will give a more accurate estimation for the expectation. Besides voting for prediction, one can also average the confidence scores from the underlying classifier for each class [44].

Adversarially Perturbed Data is used to conduct adversarial attacks and test model robustness [1]. Given an observation (\mathbf{x}, \mathbf{y}) and a trained model G , the goal is to find a point $\hat{\mathbf{x}}$ that has a small difference with \mathbf{x} and misleads G to an incorrect prediction:

$$\hat{\mathbf{x}} = \operatorname{argmax}_{\|\mathbf{x}' - \mathbf{x}\|_p \leq \epsilon} \ell_{CE}(G(\mathbf{x}'), \mathbf{y}), \quad (5)$$

where ϵ is the scale of ℓ_p -norm perturbation. Directly attacking one data point (\mathbf{x}, \mathbf{y}) without augmented smoothing operation is shown to have ill-behaved problem under randomized smoothing modeling conditions due to the argmax operator [5, 11]. We use a similar strategy to generate the adversarial samples against smoothed classifier [5].

Specifically, let $J(\mathbf{x}') = \ell_{CE}(G(\mathbf{x}'), \mathbf{y})$ be the objective function in equation 5, and G is the smoothed classifier, the empirical gradient of finding \hat{x} is given by the formula based on Monte Carlo approximations [5]:

$$\nabla_{\mathbf{x}'} J(\mathbf{x}') \approx \nabla_{\mathbf{x}'} \left(-\log \left(\frac{1}{m} \sum_{i=1}^m F(\mathbf{x}' + \delta_i)_{\mathbf{y}} \right) \right), \quad (6)$$

where m is the same hyper-parameter denoting the number of voting samples in equation 4 as well as the number of samples of Monte Carlo approximations in equation 6. We denote adversarial perturbation from equation 5 by employing Monte Carlo approximation, equation 6, as $\mathcal{A}_m^+(\mathbf{x}) = \hat{\mathbf{x}}$.

Without ambiguity, our approach only uses adversarially perturbed data $\mathcal{A}_m^+(\mathbf{x})$ in the inference stage to evaluate robust performance. In this study, PGD attack [4] and its variants [20] are used to get the practically perturbed data.

4 Robust Contrastive Learning via Randomized Smoothing

In this section, we first discuss the foundation of RUSH, an interesting yet implicit connection between contrastive learning and robustness, which suggests the existence of the *natural robustness* of contrastive learning under standard training. Such natural robustness allows us to propose a simple, yet extremely efficient and effective robust contrastive learning via randomized smoothing (RUSH). RUSH has a two-staged training process: self-supervised pre-training and supervised fine-tuning. During the pre-training stage, it uses standard training of contrastive learning, with basic noise-based data augmentation. The following fine-tuning stage and inference are empowered by the randomized smoothing paradigm, where we arm the linear classifier with label information and robust feature representation to defense adversarial attacks. The proposed RUSH algorithm is illustrated in Algorithm 1.

4.1 Natural robustness in contrastive learning

We now illustrate a key property of contrastive learning, i.e., the *natural robustness*, as a result of the implicit connection between Lipschitz continuity and the objective of contrastive learning. To see this, we will first elaborate how robustness is related to Lipschitz continuous, and then show why contrastive learning is impacting Lipschitz continuous. In the following, let f be the feature encoder of a classifier following contrastive learning framework which maps inputs $\mathcal{X} \in \mathbb{R}^d$ to feature representation in $\mathcal{Z} \in \mathbb{R}^p$. Recall that \mathcal{T} denotes a set of pre-defined data transformations in contrastive learning, $d_{\mathbf{x}}$ and $d_{\mathbf{z}}$ denote distance metrics measuring \mathbf{x}, \mathbf{z} .

Lipschitz continuity and Robustness. According to definition, if f is Lipschitz continuous, then we have the following:

$$d_{\mathbf{z}}(f(\mathbf{x}_i), f(\mathbf{x}_j)) \leq K \cdot d_{\mathbf{x}}(\mathbf{x}_i, \mathbf{x}_j), \quad (7)$$

where K is referred to as a Lipschitz constant. Since the definition holds for any $\mathbf{x}_i, \mathbf{x}_j$, we could let \mathbf{x}_j be the adversarial sample of \mathbf{x}_i . Given an original sample \mathbf{x}_i , its adversarial sample $\text{adv}(\mathbf{x}_i)$ is designed to be as close to the original as possible. Therefore, we can assume the distance between the adversarial sample and the original sample is bounded by c , and we thus have:

$$d_{\mathbf{z}}(f(\mathbf{x}_i), f(\text{adv}(\mathbf{x}_i))) \leq Kc,$$

from which we see that if a learned function or model has a small Lipschitz constant K , then the model is robust against adversarial attacks since the change in output is also bounded given small K .

Contrastive learning and Lipschitz continuity. Now recall the goal of contrastive learning, which encourages the learned feature representation from f should be similar if the input pair of images have similar content. As such, given a data point \mathbf{x} , contrastive learning in the pre-training stage embeds the following optimization objective:

$$\min_f \mathbb{E}_{\mathbf{x}_1, \mathbf{x}_2 \sim \Gamma} d_{\mathbf{z}}(f(\mathbf{x}_1), f(\mathbf{x}_2)), \quad (8)$$

where $\Gamma = \{d_{\mathbf{x}}(\mathbf{x}_1, \mathbf{x}_2) \leq c\}$ is the set of arbitrary pairs of two data points, as long as the distance between them is smaller than c . To optimize the above objective, the key question is how we get the samples from the set Γ . For example, the contrastive learning backbone of this paper (SimCLR) used a pair of transformations $t_1(\mathbf{x}), t_2(\mathbf{x})$ as the samples from Γ , where $t_1, t_2 \sim \mathcal{T}$. Therefore, we have the following objective:

$$\min_f \mathbb{E}_{\mathbf{x}_1 \sim t_1(\mathbf{x}), \mathbf{x}_2 \sim t_2(\mathbf{x})} d_{\mathbf{z}}(f(\mathbf{x}_1), f(\mathbf{x}_2)), \forall t_1, t_2 \sim \mathcal{T}. \quad (9)$$

We would like to highlight that the $d_{\mathbf{x}}$ should be treated as the distance in semantic space for the above objective. This is because although some common distance metrics for $d_{\mathbf{x}}$ such as ℓ_2 -distance cannot satisfy the distance constraint for

Algorithm 1 RUSH: robust contrastive learning via randomized smoothing

1: Require:

$\mathcal{D}, \mathcal{D}_{\text{test}}$: training and test datasets
 $f_\theta, g_{\theta_p}, \phi_{\theta_c}$: randomly initialized feature extractor, projector, and linear classifier
 \mathcal{Q} : data smoothing operation
 \mathcal{A}_m^+ : adversarially perturbing operation
 \mathcal{V}_m : voting strategy of randomized smoothing
 \mathcal{T} : pre-defined data transformation

Training: pre-training \rightarrow fine-tuning

2: repeat**3: for** (\mathbf{x}, \mathbf{y}) **in** \mathcal{D} **do**

4: $\mathbf{x}_1, \mathbf{x}_2 = t_1(\mathbf{x}), t_2(\mathbf{x})$, where $t_1, t_2 \sim \mathcal{T}$

5: $\mathbf{x}_2 = \mathcal{Q}(\mathbf{x}_2)$

6: $(\theta, \theta_p) \leftarrow (\theta, \theta_p) - \alpha \nabla_{\theta, \theta_p} \mathcal{L}_{pre}(g_{\theta_p} \circ f_\theta([\mathbf{x}_1, \mathbf{x}_2]))$

7: **end for**

8: **until** pre-training stop

9: repeat

10: **for** (\mathbf{x}, \mathbf{y}) **in** $\mathcal{D}^{[1]}$ **do**

11: $\mathbf{x} = \mathcal{Q}(\mathbf{x})$

12: $\theta_c \leftarrow \theta_c - \beta \nabla_{\theta_c} \mathcal{L}_{CE}(\phi_{\theta_c} \circ f_\theta(\mathbf{x}), \mathbf{y})^{[2]}$

13: **end for**

14: **until** fine-tuning stop

Inference: Given Input \mathbf{x}

15: $\hat{\mathbf{y}} = \mathcal{V}_m(\phi_{\theta_c} \circ f_\theta(\mathbf{x}))$

16: return $\hat{\mathbf{y}}$

Notes:

^[1] Under the transfer learning setting, \mathcal{D} and $\mathcal{D}_{\text{test}}$ come from different datasets.

^[2] The bias of the BatchNorm layers of f_θ is not frozen during fine-tuning, since batch normalization should be based on specific feature distributions, especially in the transfer learning setting.

$d_{\mathbf{x}}(t_1(\mathbf{x}), t_2(\mathbf{x}))$ for certain transformations such as rotation, there are many other valid metrics such as Wasserstein distance that satisfy the constraint.

By minimizing the objective in equation 8, we require the difference between representations to be small given similar inputs, and therefore, it is not hard to see that we are heuristically minimizing the Lipschitz constant K in equation 7. As a result, by getting a small Lipschitz constant in contrastive learning, the learned model gains robustness against adversarial attacks. And we call such robustness as *natural robustness* since it does not require additional adversarial training.

4.2 Combining Randomized Smoothing and Contrastive Learning

The natural robustness in contrastive learning delivers adversarial robustness for representation and yet we need to ensure that final classifier based on the representation is also robust. We propose integrating randomized smoothing to achieve this goal in RUSH, taking advantage of its efficiency and certified robustness. In this section, we elaborate on how the combination is done in RUSH at the pre-training, fine-tuning, and inference stages.

Pre-training. The first step is to integrate the data smoothing operation in the pre-training stage. In this end, RUSH uses the following objective function for pre-training:

$$\min_{\theta, \theta_p} \mathbb{E}_{t_1, t_2 \sim \mathcal{T}, \mathbf{x} \in \mathcal{D}} \mathcal{L}_{pre}(g_{\theta_p} \circ f_\theta([t_1(\mathbf{x}), \mathcal{Q}(t_2(\mathbf{x}))])), \quad (10)$$

where \mathcal{L}_{pre} is NT-Xent loss following the original definition from [17], and \mathcal{Q} is our selected randomized smoothing operation to the data as in equation 3, which can be considered as entity-wise noising the input. We note that different from the original SimCLR, there is no need to apply Gaussian blur in \mathcal{T} , since we already have our data smoothing operation \mathcal{Q} . More details can be found at Appendix A.

Fine-tuning. Next, we embed data smoothing operation into fine-tuning stage to extract the robust feature representations. As such, RUSH used the following objective for the fine-tuning stage:

$$\min_{\theta_c} \mathbb{E}_{\mathbf{x}, \mathbf{y} \in \mathcal{D}} \mathcal{L}_{CE}(\phi_{\theta_c} \circ f_{\theta}(\mathcal{Q}(\mathbf{x})), \mathbf{y}), \quad (11)$$

where \mathcal{Q} is the same data smoothing operation. Unless otherwise specified, we use the same smoothing distribution as the one used for pre-training, fine-tuning and inference.

Inference. Besides the treatments in training, RUSH uses adversarial perturbation \mathcal{A}_m^+ in equation 6 and voting strategy \mathcal{V}_m in equation 4, as illustrated in Algorithm 1.

We note that in typical randomized smoothing settings, the value of m is set to a reasonable value (e.g., 32, 64, or 128) and sometimes it varies across samples for the fixed certificated radius. From our empirical study, we find that RUSH also delivers rather promising performance when $m = 1$. Since $m = 1$ represents the situation of maximum computational efficiency of our approach. Under this inference strategy, RUSH has no extra computational overhead as compared to the vanilla SimCLR algorithm in both training and inference stages. So, unless otherwise specified, there are two test strategies in this study, \mathcal{I}_F^+ and \mathcal{I}_F , with different hyper-parameter m . Specifically, \mathcal{I}_F denotes using $m = 1$ for \mathcal{A}_m^+ and \mathcal{V}_m . \mathcal{I}_F^+ denotes using $m > 1$ for \mathcal{A}_m^+ and \mathcal{V}_m , e.g., $m = 64$.

5 Experiments

In this section, we demonstrate the effectiveness of our proposed RUSH from two aspects: (a) Performance comparison between RUSH and other key related approaches including cross-datasets and cross-tasks robustness against PGD attacks [4] and AA attacks [20]; (b) Qualitative results including robustness evaluation at various levels of PGD attack strengths and impact of the noise level of smoothing distribution.

5.1 Setup

The RUSH algorithm can be applied to a variety of machine learning and data mining problems with general structured data. As many competing approaches used image datasets for evaluation, we will follow this evaluation scheme. Specifically, we conduct experiments on three image benchmark datasets, CIFAR-10, CIFAR-100, and STL10, with two robustness evaluation metrics, standard accuracy over original images without perturbations and robust accuracy over adversarially perturbed images via first-order methods including PGD attack and AA attack.

We use ResNet-18 for the encoder architecture of f_{θ} , a two-layer MLP projection head g_{θ_p} to project the representation, and one linear layer for linear classifier ϕ_{θ_c} . For image transformation \mathcal{T} , we use random resized crop, random horizontal flip, and color distortions. Detailed implementations are provided in Appendix A. Unless otherwise specified, we use uniform distribution $\delta \sim U_{32 \times 32}(-0.3, 0.3)$ as our default smoothing distribution.

Training Setting. Recall that the proposed RUSH has a two-stage training process. (i) In the *pre-training* stage, model $g_{\theta_p} \circ f_{\theta}$ is trained with a SGD optimizer with batch size=512, initial learning rate=0.5, momentum=0.9, and weight decay=0.0001 for 1000 epochs. We use cosine learning rate decay during training with minimum learning rate = 0.001. The temperature parameter in contrastive loss \mathcal{L}_{pre} is set to 0.5. (ii) In the *fine-tuning* stage, model $\phi_{\theta_c} \circ f_{\theta}$ is trained with the frozen feature extractor f_{θ} . We note that as we believe batch normalization should be based on specific feature distributions, so the bias of the BatchNorm layers of f_{θ} is not frozen during fine-tuning. We use a SGD optimizer with batch size=512, initial learning rate=0.1, momentum=0.9, and weight decay=0.0002 to train the network for 25 epochs. We use cosine learning rate decay during training with minimum learning rate = 0.001.

Inference Setting. Standard accuracy and robust accuracy are evaluated with clean data and perturbed data respectively under two inference strategies described in Section 4.2. Unless otherwise specified, we use $m = 64$ for the inference strategy \mathcal{I}_F^+ , i.e., 64 number of sampling for both adversarial perturbation \mathcal{A}_m^+ and voting strategy \mathcal{V}_m . \mathcal{I}_F is always with $m = 1$.

For adversarial perturbation, unless otherwise specified, we use ℓ_{∞} -norm PGD attack with 20 steps and 8/255 maximum perturbation as our default PGD setting. Robustness performance at various PGD attack strengths over steps $\in \{20, 40, 80\}$ and maximum perturbation $\in \{8/255, 16/255, 32/255\}$ are also evaluated independently, as shown in Table 2. We use the standard version ℓ_{∞} -norm AA attack with 8/255 maximum perturbation. We use the library TORCHATTACKS [45] for all the adversarial attacks.

Without ambiguity, inference strategy \mathcal{I}_F^+ and \mathcal{I}_F with adversarial perturbation \mathcal{A}_m^+ are designed for smoothed classifiers with stronger attack strength to our model [5]. During the inference of our approach, the attacks to our model including PGD attack and AA attack are re-implemented with noise-based augmentation according to equation 6.

Table 1: Performance comparison over baselines, in terms of standard accuracy, robust accuracy under $\ell_\infty=8/255$ PGD and $\ell_\infty=8/255$ AA attacks with ResNet-18 on CIFAR-10, CIFAR-100, CIFAR-10 \rightarrow STL-10, and STL-10 \rightarrow STL-10. The top performance is highlighted in bold.

Dataset	Methods	Acc.(%)		
		Standard	PGD	AA
CIFAR-10	RUSH \mathcal{I}_F^+ (ours)	87.9	77.8	79.5
	RUSH \mathcal{I}_F (ours)	86.4	73.7	74.7
	RoCL [30]	83.7	40.2	-
	Free-m [27]	85.9	46.8	-
	AdvCL [46]	83.6	52.7	49.7
	SmoothAdv Training[5] ⁴	86.2	68.2	-
	ACL [6] ¹	82.5	52.8	49.3
	Data AUG [47] ¹	83.5	59.9	57.0
	Data AUG [47] ²	92.2	-	66.5
CIFAR-100	RUSH \mathcal{I}_F^+ (ours)	57.1	46.6	-
	RUSH \mathcal{I}_F (ours)	55.3	42.5	40.2
	AdvCL [46]	56.7	28.7	24.7
	Data AUG [47] ¹	56.9	32.0	28.5
	Data AUG [47] ²	63.5	-	34.6
CIFAR-10 \rightarrow STL-10	RUSH \mathcal{I}_F^+ (ours)	73.7	53.3	55.9
	RUSH \mathcal{I}_F (ours)	72.0	49.4	53.4
	BYORL [14]	-	24.1	-
	AdvCL [46]	63.5	37.7	34.7
STL-10 ³	RUSH \mathcal{I}_F^+ (ours)	76.7	64.6	67.0
\rightarrow STL-10	RUSH \mathcal{I}_F (ours)	75.1	61.5	60.2

¹ using the provided pre-trained ResNet18 model and testing on our pipeline.

² latest state-of-the-art according to [48] (Link: <https://robustbench.github.io/index.html>), which applied network architecture WideResNet-70-16. The standard accuracy marked as ² will not be ranked considering fair comparisons.

³ STL-10 denotes the independent set of unlabeled examples in STL-10. Most existing robust models use label information to generate adversarial examples for robust training, so baseline using STL-10 is few.

⁴ under $\ell_\infty=2/255$ PGD attack with ResNet-110.

5.2 Performance

Overall cross-datasets and cross-tasks performance. Table 1 summarizes the performance of our approach under inference strategy \mathcal{I}_F^+ and \mathcal{I}_F and key competing baselines over CIFAR-10, CIFAR100, CIFAR-10 \rightarrow STL-10, and STL-10 unlabeled \rightarrow STL-10, where \rightarrow denotes transfer learning setting, e.g., CIFAR-10 \rightarrow STL-10 means the model is pre-trained on the training set of CIFAR-10, fine-tuned on the training set of STL-10, and tested on the test set of STL-10.

We see that the proposed RUSH outperforms all competing baselines w.r.t. both standard accuracy and robust accuracy under network architecture ResNet-18 in all settings. Compared with state-of-the-arts using network architecture WideResNet-70-16, RUSH still outperforms them with a significant margin on robust accuracy. The method SmoothAdv Training uses smoothed classifier to defend first-order-based attacks [5], which uses a similar intuition as ours. However, RUSH outperforms it with less complexity of network architecture and regardless of adversarial examples.

We note that the idea of RUSH can be practically extended to other SSL frameworks other than SimCLR, such as BYOL [18]. See Appendix B.

Robustness evaluation at various attack strengths. We evaluate the model performance at various PGD attack strengths over steps $\in \{20, 40, 80\}$, ℓ_∞ -norm maximum perturbation $\in \{8/255, 16/255, 32/255\}$, and ℓ_2 -norm maximum perturbation $\in \{0.25, 0.5, 1.0, 1.5, 2.0\}$. Results are shown in Table 2. We note that there exist saturated attack steps for a certain maximum perturbation considering PGD attack is first-order method operating on data and

Table 2: Top-1 accuracy of our classifier on CIFAR-10 under PGD attack with various maximum perturbation and attack steps.

Distance Measure	Maximum Perturbation	Acc.(%) with Steps					
		Under \mathcal{I}_F^+			Under \mathcal{I}_F		
		20	40	80	20	40	80
ℓ_∞	8/255	77.5	78.0	78.3	73.6	74.2	74.6
	16/255	67.5	68.8	69.7	56.8	57.8	58.3
	32/255	62.6	57.7	56.7	35.2	27.9	26.6
ℓ_2	0.25	87.5	87.5	87.4	86.1	85.9	85.8
	0.5	86.9	86.8	86.7	85.3	85.2	85.0
	1.0	84.8	84.9	85.3	82.3	82.6	83.0
	1.5	80.9	81.8	82.4	77.4	77.8	78.4
	2.0	77.6	77.2	78.5	72.0	70.5	72.4

gradients. Attack with restricted attack steps may generate adversarial examples that do not reach the maximum perturbation, and attack with over saturated attack steps will not generate stronger adversarial examples.

For ℓ_∞ -norm maximum perturbation, the results in Table 2 can be understood from two perspectives, maximum perturbation and the number of PGD steps:

(a) With the maximum perturbation increasing, the robust accuracy of our model decreases. We focus on the setting of 80 steps, which we believe is close to saturated attack steps considering the similar performance of 40 steps and 80 steps. Changing the maximum perturbation from 8/255 to 16/255, there is about 8% drop in accuracy under \mathcal{I}_F^+ . From 16/255 to 32/255, there is about 13% drop in accuracy under \mathcal{I}_F^+ . Under inference strategy \mathcal{I}_F where the number of Monte-Carlo sampling $m = 1$, the robust accuracy decreases with a large margin at about 16% and 32% over $\ell_\infty = 8/255$ to $\ell_\infty = 16/255$ and $\ell_\infty = 16/255$ to $\ell_\infty = 32/255$.

(b) We see a larger number of PGD steps fails to influence the robust accuracy of our model with 8/255 and 16/255 maximum perturbation and has very limited influence with 32/255 maximum perturbation. An explanation is that if the perturbation is bounded in a small value (8/255 and 16/255), the corresponding saturated attack steps are small, so the robust accuracy does not change along with steps increasing. However, if the perturbation is bounded in a relatively larger value (32/255), it requires more attack steps to reach maximum perturbation.

For ℓ_2 -norm maximum perturbation, we see that our model is robust to ℓ_2 -norm PGD attack with maximum perturbation $\in \{0.25, 0.5, 1.0, 1.5, 2.0\}$. With the maximum perturbation varying from $\ell_2 = 0.25$ to 2.0 under \mathcal{I}_F^+ , there is only $\sim 10\%$ drop in robust accuracy.

We also highlight that RUSH provides consistent robustness against ℓ_2 and ℓ_∞ attacks. There are two factors that affect the robustness performance, the amount of total perturbation and the attack methods. To investigate the effects of different attack methods, we focus on $\ell_2 = 2.0$ and $\ell_\infty = 8/255$ settings since the total perturbation of these two settings are similar ($(9/255)\sqrt{3} * 32^2 \approx 2$), and therefore we can focus on the difference of attacking methods. As seen in the first row and last row of Table 2, the robust performance of ℓ_∞ attack is similar to that of ℓ_2 attack, which suggests that RUSH mitigates the differences among ℓ_2 and ℓ_∞ attacks.

Considering it is white-box attack, it will be unfair comparisons if we report our model performance under attacks without noise-based augmentation on \mathcal{A}_m^+ . However, we believe our model performance, under attacks and without noise-based augmentation, is still meaningful in real-world applications. The results can be found in Table 3. We see that when the attacks are directly applied to the original data without noising, robust accuracy reaches about 86% under the attack setting $\ell_\infty = 8/255$, which is close to the standard accuracy 87.8%. And under various strengths of ℓ_2 -norm PGD attacks, our model shows a limited accuracy drop.

Transferable Attack Performance. To evaluate how different methods perform against transferable attacks, we select two other common competing algorithms besides RUSH, (i.e. ACL [6] and DataAUG [47]) and evaluate the model performance by exchanging the generated adversarial examples. First, we see that all four methods give the worst robustness performance (i.e. lowest PGD accuracy and AA accuracy) against the attack which is designed against themselves. Moreover, RUSH achieves the best performance testing with adversarial examples generated by Data AUG and the best robust accuracy under AA attacks with adversarial examples generated by ACL. This indicates the robustness of RUSH is transferable among different types of adversarial samples, which makes RUSH applicable to other transferable adversarial attacks.

Table 3: Top-1 accuracy of our classifier on CIFAR-10 under common PGD attack with various maximum perturbation and attack steps - without noise-based augmentation in \mathcal{A}_m^+ .

Dataset	Distance Measure	Maximum Perturbation	Acc.(%) with Steps		
			20	40	80
CIFAR-10	ℓ_∞	8/255	86.2	86.1	86.1
		16/255	80.7	79.1	78.7
		32/255	50.2	39.3	32.5
	ℓ_2	0.25	87.7	87.7	87.7
		0.5	87.5	87.3	87.6
		1.0	86.5	86.6	86.8
		1.5	85.0	85.0	85.5
		2.0	84.0	82.7	82.9

Table 4: Transferable Attack Performance comparison, in terms of standard accuracy, robust accuracy under $\ell_\infty=8/255$ PGD and $\ell_\infty=8/255$ AA attacks on CIFAR-10. The top performance is highlighted in bold.

Adv-examples generated by	Methods	Acc.(%)		
		Standard	PGD	AA
ACL [6]	RUSH \mathcal{I}_F^+ (ours)	87.8	62.3	72.8
	RUSH \mathcal{I}_F (ours)	86.4	60.4	71.7
	ACL [6]	82.5	52.8	49.3
	Data AUG [47]	83.6	67.7	71.3
Data AUG [47]	RUSH \mathcal{I}_F^+ (ours)	87.9	64.3	75.6
	RUSH \mathcal{I}_F (ours)	86.4	63.0	67.0
	ACL [6]	82.4	63.1	67.2
	Data AUG [47]	83.5	59.9	57.0
RUSH \mathcal{I}_F^+ (ours)	RUSH \mathcal{I}_F^+ (ours)	87.9	79.9	80.5
	ACL [6]	82.3	77.8	79.5
	Data AUG [47]	83.5	81.4	82.0
RUSH \mathcal{I}_F (ours)	RUSH \mathcal{I}_F (ours)	86.4	73.8	74.3
	ACL [6]	82.4	79.5	79.9
	Data AUG [47]	83.6	81.0	81.3

5.3 Ablation Study

Firstly, we evaluate the model performance when RUSH applies various noise levels of smoothing distribution. Secondly, since our approach combines contrastive learning with randomized smoothing, we evaluate the model performance when applying different randomized smoothing strategies in RUSH. Finally, we describe the performance difference between the supervised pre-trained model and the model pre-trained by RUSH.

Effect of the noise level of smoothing distribution. There are two critical components in randomized smoothing: the choice of the smoothing distribution and the noise level of smoothing distribution. Using uniform distribution to train a smoothed classifier against ℓ_∞ -norm perturbation, which is the focus in this study, is considered to be a reasonable choice, and we study the performance of RUSH applying various noise levels of smoothing distribution (uniform distribution).

We vary the range of uniform distribution to evaluate the performance of our model on CIFAR-10 and CIFAR-10 \rightarrow STL-10, and the results are shown in Table 5. With a small noise level, $\mu=0.1$, the model has the best standard accuracy and the lowest robust accuracy with a significant margin with the robust accuracy applying other noise levels.

However, in Table 5, the last three rows vary $\mu \in \{0.3, 0.5, 0.7\}$ for the two conditions, CIFAR-10 and CIFAR-10 \rightarrow STL-10. We see that both standard accuracy and robust accuracy are stable. Under settings of dataset CIFAR-10, noise level $\mu = 0.3$, and \mathcal{I}_F^+ , standard accuracy and robust accuracy achieve 87.8% and 77.4%, respectively. The standard accuracy is close to the result training with pure SimCLR 92.6% meanwhile the model keeps a relatively high

Table 5: Sensitivity analysis: RUSH applying various noise level μ of data smoothing operation $\mathcal{Q}(x) = x + \delta$ where $\delta \sim U_{n \times d}(-\mu, \mu)$ under 20 steps $\ell_\infty=8/255$ PGD attack.

Dataset	Noise level μ	Acc.(%)			
		Under \mathcal{I}_F^+		Under \mathcal{I}_F	
		Standard	PGD	Standard	PGD
CIFAR-10	0.1	88.9	26.1	88.2	20.6
	0.3	87.8	77.4	86.4	73.7
	0.5	86.7	83.3	84.2	79.3
	0.7	85.5	85.0	82.0	80.3
CIFAR-10 →STL-10	0.1	74.7	26.1	74.1	16.5
	0.3	73.6	53.6	72.0	49.4
	0.5	71.5	65.0	69.4	61.8
	0.7	70.3	67.8	67.3	65.1

Table 6: RUSH applying randomized smoothing with different strategies on CIFAR-10 under 20 steps $\ell_\infty=8/255$ PGD attack.

Data smoothing in		Test Strategy	Acc.(%)	
Pre-training	Fine-tuning		Standard	PGD
f_θ is pre-trained with Contrastive Learning				
No	No	common ^[1]	92.6	0.0
No	Yes	\mathcal{I}_F^+	87.2	67.8
Yes	Yes	\mathcal{I}_F^+	87.8	77.5
No	Yes	\mathcal{I}_F	82.9	58.3
Yes	Yes	\mathcal{I}_F	86.4	73.7
f_θ is pre-trained on CIFAR-10 with Supervised Learning				
No	No	common	87.6	0.1
No	Yes	\mathcal{I}_F^+	65.4	37.6
Yes	Yes	\mathcal{I}_F^+	63.6	51.0

¹ denotes without using voting strategy and noise-based data smoothing operation for adversarial perturbation in test.

robust accuracy. Only increasing the μ to 0.7, the model keeps standard accuracy at 85.5% and almost eliminate the gap between standard accuracy and robust accuracy.

As such, we see that our approach is not sensitive with the scale of the noise level of the smoothing distribution, if the noise level is reasonably selected according to the range of image data that scale to (0, 1).

Effect of randomized smoothing strategies on RUSH. Firstly, we focus on the three settings corresponding to the first three rows in Table 6: (a) Pure SimCLR training and test setting, (b) Applying data smoothing operation on the fine-tuning stage with randomized smoothing voting strategy during inference, and (c) The proposed RUSH which applies smoothing operation on both pre-training and fine-tuning stages with randomized smoothing voting strategy.

Compared the first row with the second row in Table 6, both of them have the same pre-training model, and we can see the robust accuracy increased from 0.0% to 67.8% in the meanwhile the standard accuracy only decreased from 92.6% to 87.2% by applying the randomized smoothing (applying data smoothing on fine-tuning stage and applying voting during inference). This indicates the model can acquire significant robustness to PGD attack and keep a high standard accuracy by cooperating contrastive learning with randomized smoothing. We see that the robust accuracy increased from 67.8% at row-2 to 77.5% at row-3 by applying both image transformation and data smoothing operation on the pre-training stage. This suggests that better smoothing the input data of the contrastive learning can significantly improve the robustness of the pre-trained model.

Besides, we see surprisingly that our approach is not sensitive to the number of Monte-Carlo sampling in the inference of randomized smoothing. Changing the number of sampling from 64 to only 1, the robust accuracy only decreased from 77.5% at row-3 to 73.7% at row-5 and the standard accuracy only decreased from 87.8% at row-3 to 86.4% at row-5. This is because we are using empirical mean to estimate the expectation of a bounded random variable (i.e.,

from 0 to 1), which enjoys the sub-Gaussian convergence rate. Empirically we found that increasing m beyond 16 did not further improve performance referring Table 7.

Table 7: Top-1 accuracy of the classifier by RUSH with varying number of Monte-Carlo sampling under $\ell_\infty=8/255$ PGD attacks on CIFAR-10.

Type of accuracy	Acc.(%) with varying number of sampling					
	1	8	16	32	64	128
Standard	86.1	87.6	87.8	87.8	87.8	87.9
Robust	73.1	76.8	77.3	77.3	77.4	77.4

Comparing with Common Randomized Smoothing Method. In the last three row of Table 6, we replace the model pre-trained by contrastive learning with the model pre-trained with supervised learning. Without data smoothing in pre-training, the standard accuracy of the supervised learning model decreases from 87.6% at row-6 to 65.4% at row-7, and the robust accuracy increases from 0.1% at row-6 to 37.6% at row-7. By applying data smoothing operation on the pre-training stage, the standard accuracy of the supervised learning model decreases slightly from 65.4% at row-7 to 63.6% at row-8, and the robust accuracy increases from 37.6% at row-7 to 51.0% at row-8. Comparing row-3 and row-8 in Table 6, there are over 20% increasing in both standard accuracy and robust accuracy. It is clear that natural robustness introduced by contrastive learning boost the smoothed classifier in terms of both standard accuracy and robust accuracy.

To demonstrate the effectiveness of our approach, in Figure 1 and Figure 2, we visualize the learned feature representations over models pre-trained by contrastive learning and supervised learning on CIFAR-10, using t-SNE [49]. Each point is colored with its ground-truth label.

Figure 1(a) shows the feature representation of the original images obtained by CL. We see that Figure 1(a) does not have clear class boundary, since label information and noised images are only associated in finetuning stage. Figure 1(b) is the feature representation of the original images obtained by SL. We see that, different from Figure 1(a), Figure 1(b) has a relatively clearer class boundary, since label information and noised images are associated in pre-training stage.

Figure 2(a) and Figure 2(b) stand for the feature representation of obtaining standard accuracy and robust accuracy at row-3 in Table 6 where the model is pre-trained with contrastive learning. Figure 2(c) and Figure 2(d) stand for the feature representation of obtaining standard accuracy and robust accuracy at row-8 in Table 6 where the model is pre-trained with supervised learning. Comparing the difference between Figure 2(c) and Figure 2(d) and the difference between Figure 2(a) and Figure 2(b), the perturbation shifts the feature representation of SL larger than the feature representation learned by our approach, where the comparison details are highlighted with black box in Figure 2. It shows the effectiveness of the proposed approach against perturbation.

We believe the weak association between label information and feature representation learned by the proposed approach is one of the reasons helping our model against first-order-based attacks. However, comparing row-3 and row-8 in Table 6, we have not explicated the difference between the robust feature representation learned by supervised learning and the robust feature representation learned by contrastive learning which we believe contains natural Lipschitz regularization. We leave a principled analysis exploring how the robust feature representation learned by RUSH boosts the smoothed classifier to future work.

6 Conclusions

In this paper, we designed a robust contrastive learning algorithm RUSH by exploring the natural robustness in contrastive learning. We showed that RUSH maintains a high standard accuracy and substantially improves robust accuracy. Extensive empirical studies showed that RUSH outperforms all existing ℓ_∞ -robust methods by a significant margin on common image benchmarks including CIFAR-10, CIFAR-100, and STL-10.

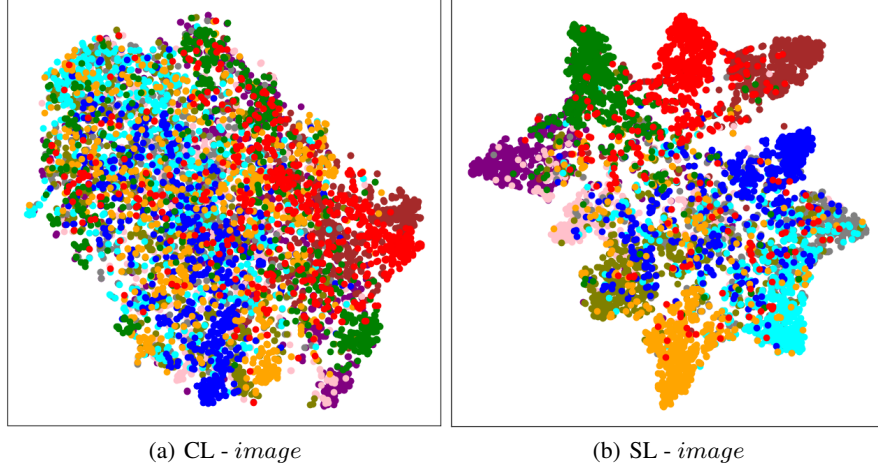


Figure 1: Learned feature representations of Contrastive Learning (CL) and Supervised Learning (SL) on CIFAR-10 over original images.

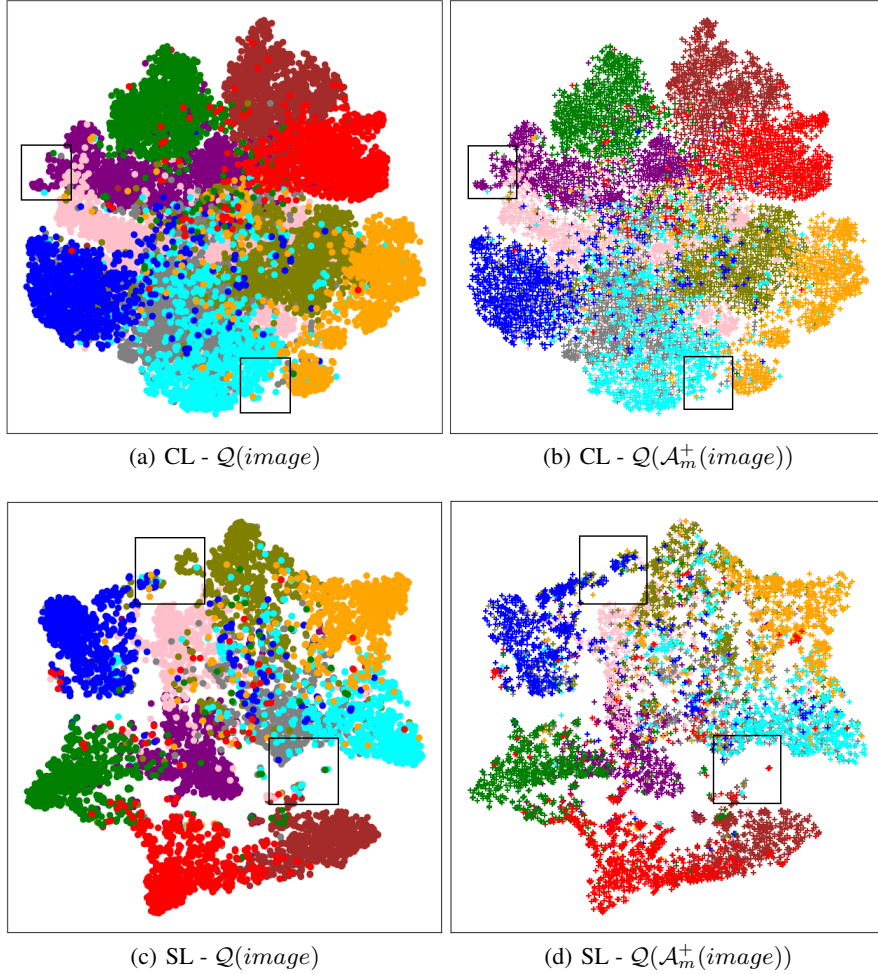


Figure 2: Learned feature representations of contrastive learning and supervised learning on CIFAR-10 over noised images $\mathcal{Q}(\text{image})$ and noised perturbed images $\mathcal{Q}(\mathcal{A}_m^+(\text{image}))$. To compare the shift of feature representation introduced by adversarial perturbation, $\mathcal{Q}(\text{image}) \rightarrow \mathcal{Q}(\mathcal{A}_m^+(\text{image}))$, the difference is highlighted with black boxes. A smaller difference between left figure and right figure indicates more robust representation.

References

- [1] Ian J Goodfellow, Jonathon Shlens, and Christian Szegedy. Explaining and harnessing adversarial examples. *arXiv preprint arXiv:1412.6572*, 2014.
- [2] Naveed Akhtar and Ajmal Mian. Threat of adversarial attacks on deep learning in computer vision: A survey. *Ieee Access*, 6:14410–14430, 2018.
- [3] Harini Kannan, Alexey Kurakin, and Ian Goodfellow. Adversarial logit pairing. *arXiv preprint arXiv:1803.06373*, 2018.
- [4] Aleksander Madry, Aleksandar Makelov, Ludwig Schmidt, Dimitris Tsipras, and Adrian Vladu. Towards deep learning models resistant to adversarial attacks. *arXiv preprint arXiv:1706.06083*, 2017.
- [5] Hadi Salman, Jerry Li, Ilya Razenshteyn, Pengchuan Zhang, Huan Zhang, Sebastien Bubeck, and Greg Yang. Provably robust deep learning via adversarially trained smoothed classifiers. *Advances in Neural Information Processing Systems*, 32, 2019.
- [6] Ziyu Jiang, Tianlong Chen, Ting Chen, and Zhangyang Wang. Robust pre-training by adversarial contrastive learning. *Advances in Neural Information Processing Systems*, 33:16199–16210, 2020.
- [7] Alexey Kurakin, Ian Goodfellow, and Samy Bengio. Adversarial machine learning at scale. *arXiv preprint arXiv:1611.01236*, 2016.
- [8] Anish Athalye, Nicholas Carlini, and David Wagner. Obfuscated gradients give a false sense of security: Circumventing defenses to adversarial examples. In *International conference on machine learning*, pages 274–283. PMLR, 2018.
- [9] Aditi Raghunathan, Jacob Steinhardt, and Percy S Liang. Semidefinite relaxations for certifying robustness to adversarial examples. *Advances in Neural Information Processing Systems*, 31, 2018.
- [10] Eric Wong and Zico Kolter. Provable defenses against adversarial examples via the convex outer adversarial polytope. In *International Conference on Machine Learning*, pages 5286–5295. PMLR, 2018.
- [11] Jeremy Cohen, Elan Rosenfeld, and Zico Kolter. Certified adversarial robustness via randomized smoothing. In *International Conference on Machine Learning*, pages 1310–1320. PMLR, 2019.
- [12] Dan Hendrycks, Mantas Mazeika, Saurav Kadavath, and Dawn Song. Using self-supervised learning can improve model robustness and uncertainty. *arXiv preprint arXiv:1906.12340*, 2019.
- [13] Jean-Baptiste Alayrac, Jonathan Uesato, Po-Sen Huang, Alhussein Fawzi, Robert Stanforth, and Pushmeet Kohli. Are labels required for improving adversarial robustness? *Advances in Neural Information Processing Systems*, 32, 2019.
- [14] Sven Gowal, Po-Sen Huang, Aaron van den Oord, Timothy Mann, and Pushmeet Kohli. Self-supervised adversarial robustness for the low-label, high-data regime. In *International Conference on Learning Representations*, 2020.
- [15] Longlong Jing and Yingli Tian. Self-supervised visual feature learning with deep neural networks: A survey. *IEEE transactions on pattern analysis and machine intelligence*, 43(11):4037–4058, 2020.
- [16] Kaiming He, Haoqi Fan, Yuxin Wu, Saining Xie, and Ross Girshick. Momentum contrast for unsupervised visual representation learning. In *Proceedings of the IEEE/CVF conference on computer vision and pattern recognition*, pages 9729–9738, 2020.
- [17] Ting Chen, Simon Kornblith, Mohammad Norouzi, and Geoffrey Hinton. A simple framework for contrastive learning of visual representations. In *International conference on machine learning*, pages 1597–1607. PMLR, 2020.
- [18] Jean-Bastien Grill, Florian Strub, Florent Altché, Corentin Tallec, Pierre Richemond, Elena Buchatskaya, Carl Doersch, Bernardo Avila Pires, Zhaohan Guo, Mohammad Gheshlaghi Azar, et al. Bootstrap your own latent—a new approach to self-supervised learning. *Advances in Neural Information Processing Systems*, 33:21271–21284, 2020.
- [19] Tianlong Chen, Sijia Liu, Shiyu Chang, Yu Cheng, Lisa Amini, and Zhangyang Wang. Adversarial robustness: From self-supervised pre-training to fine-tuning. In *Proceedings of the IEEE/CVF Conference on Computer Vision and Pattern Recognition*, pages 699–708, 2020.
- [20] Francesco Croce and Matthias Hein. Reliable evaluation of adversarial robustness with an ensemble of diverse parameter-free attacks. In *International conference on machine learning*, pages 2206–2216. PMLR, 2020.
- [21] Alex Krizhevsky, Geoffrey Hinton, et al. Learning multiple layers of features from tiny images. 2009.

- [22] Adam Coates, Andrew Ng, and Honglak Lee. An analysis of single-layer networks in unsupervised feature learning. In *Proceedings of the fourteenth international conference on artificial intelligence and statistics*, pages 215–223. JMLR Workshop and Conference Proceedings, 2011.
- [23] Seyed-Mohsen Moosavi-Dezfooli, Alhussein Fawzi, and Pascal Frossard. Deepfool: a simple and accurate method to fool deep neural networks. In *Proceedings of the IEEE conference on computer vision and pattern recognition*, pages 2574–2582, 2016.
- [24] Nicolas Papernot, Patrick McDaniel, Xi Wu, Somesh Jha, and Ananthram Swami. Distillation as a defense to adversarial perturbations against deep neural networks. In *2016 IEEE symposium on security and privacy (SP)*, pages 582–597. IEEE, 2016.
- [25] Nicholas Carlini and David Wagner. Towards evaluating the robustness of neural networks. In *2017 IEEE symposium on security and privacy (SP)*, pages 39–57. IEEE, 2017.
- [26] Weilin Xu, David Evans, and Yanjun Qi. Feature squeezing: Detecting adversarial examples in deep neural networks. *arXiv preprint arXiv:1704.01155*, 2017.
- [27] Ali Shafahi, Mahyar Najibi, Mohammad Amin Ghiasi, Zheng Xu, John Dickerson, Christoph Studer, Larry S Davis, Gavin Taylor, and Tom Goldstein. Adversarial training for free! *Advances in Neural Information Processing Systems*, 32, 2019.
- [28] Eric Wong, Leslie Rice, and J Zico Kolter. Fast is better than free: Revisiting adversarial training. *arXiv preprint arXiv:2001.03994*, 2020.
- [29] Dinghuai Zhang, Tianyuan Zhang, Yiping Lu, Zhanxing Zhu, and Bin Dong. You only propagate once: Accelerating adversarial training via maximal principle. *Advances in Neural Information Processing Systems*, 32, 2019.
- [30] Minseon Kim, Jihoon Tack, and Sung Ju Hwang. Adversarial self-supervised contrastive learning. *Advances in Neural Information Processing Systems*, 33:2983–2994, 2020.
- [31] Guy Katz, Clark Barrett, David L Dill, Kyle Julian, and Mykel J Kochenderfer. Reluplex: An efficient smt solver for verifying deep neural networks. In *International Conference on Computer Aided Verification*, pages 97–117. Springer, 2017.
- [32] Vincent Tjeng, Kai Xiao, and Russ Tedrake. Evaluating robustness of neural networks with mixed integer programming. *arXiv preprint arXiv:1711.07356*, 2017.
- [33] Timon Gehr, Matthew Mirman, Dana Drachler-Cohen, Petar Tsankov, Swarat Chaudhuri, and Martin Vechev. Ai2: Safety and robustness certification of neural networks with abstract interpretation. In *2018 IEEE Symposium on Security and Privacy (SP)*, pages 3–18. IEEE, 2018.
- [34] Matthew Mirman, Timon Gehr, and Martin Vechev. Differentiable abstract interpretation for provably robust neural networks. In *International Conference on Machine Learning*, pages 3578–3586. PMLR, 2018.
- [35] Lily Weng, Huan Zhang, Hongge Chen, Zhao Song, Cho-Jui Hsieh, Luca Daniel, Duane Boning, and Inderjit Dhillon. Towards fast computation of certified robustness for relu networks. In *International Conference on Machine Learning*, pages 5276–5285. PMLR, 2018.
- [36] Xuanqing Liu, Minhao Cheng, Huan Zhang, and Cho-Jui Hsieh. Towards robust neural networks via random self-ensemble. In *Proceedings of the European Conference on Computer Vision (ECCV)*, September 2018.
- [37] Xiaoyu Cao and Neil Zhenqiang Gong. Mitigating evasion attacks to deep neural networks via region-based classification. In *Proceedings of the 33rd Annual Computer Security Applications Conference*, pages 278–287, 2017.
- [38] Jiaye Teng, Guang-He Lee, and Yang Yuan. ℓ_1 adversarial robustness certificates: a randomized smoothing approach. 2019.
- [39] Dinghuai Zhang, Mao Ye, Chengyue Gong, Zhanxing Zhu, and Qiang Liu. Filling the soap bubbles: Efficient black-box adversarial certification with non-gaussian smoothing. 2019.
- [40] Alexander Levine and Soheil Feizi. Robustness certificates for sparse adversarial attacks by randomized ablation. In *Proceedings of the AAAI Conference on Artificial Intelligence*, volume 34, pages 4585–4593, 2020.
- [41] Greg Yang, Tony Duan, J Edward Hu, Hadi Salman, Ilya Razenshteyn, and Jerry Li. Randomized smoothing of all shapes and sizes. In *International Conference on Machine Learning*, pages 10693–10705. PMLR, 2020.
- [42] Dimitris Tsipras, Shibani Santurkar, Logan Engstrom, Alexander Turner, and Aleksander Madry. Robustness may be at odds with accuracy. *arXiv preprint arXiv:1805.12152*, 2018.

- [43] Mathias Lecuyer, Vaggelis Atlidakis, Roxana Geambasu, Daniel Hsu, and Suman Jana. Certified robustness to adversarial examples with differential privacy. In *2019 IEEE Symposium on Security and Privacy (SP)*, pages 656–672. IEEE, 2019.
- [44] Aounon Kumar, Alexander Levine, Soheil Feizi, and Tom Goldstein. Certifying confidence via randomized smoothing. *Advances in Neural Information Processing Systems*, 33:5165–5177, 2020.
- [45] Hoki Kim. Torchattacks: A pytorch repository for adversarial attacks. *arXiv preprint arXiv:2010.01950*, 2020.
- [46] Lijie Fan, Sijia Liu, Pin-Yu Chen, Gaoyuan Zhang, and Chuang Gan. When does contrastive learning preserve adversarial robustness from pretraining to finetuning? *Advances in Neural Information Processing Systems*, 34, 2021.
- [47] Sylvestre-Alvise Rebuffi, Sven Gowal, Dan A Calian, Florian Stimberg, Olivia Wiles, and Timothy Mann. Fixing data augmentation to improve adversarial robustness. *arXiv preprint arXiv:2103.01946*, 2021.
- [48] Francesco Croce, Maksym Andriushchenko, Vikash Sehwal, Edoardo Debenedetti, Nicolas Flammarion, Mung Chiang, Prateek Mittal, and Matthias Hein. Robustbench: a standardized adversarial robustness benchmark. *arXiv preprint arXiv:2010.09670*, 2020.
- [49] Laurens Van der Maaten and Geoffrey Hinton. Visualizing data using t-sne. *Journal of machine learning research*, 9(11), 2008.

A Details of Image Transformation

We provide the full code in the supplementary materials for reproducing the results. Here we elaborate the details of image transformations used in the paper, a key part of our implementation. We utilize *random resized crop*, *random horizontal flip*, and *random color distortion* as the default image transformation. Different from the original data augmentation of SimCLR, we do not apply random Gaussian blur, as discussed in Section 4.2.

The operation constructing a pair of transformed images are detailed as below. We note that:

- $\mathcal{T}(x)$ is `T_simCLR(img, flag_RdSm = False)`
- $\mathcal{Q}(\mathcal{T}(x))$ is `T_simCLR(img, flag_RdSm = True)`

```
import torchvision
T_simCLR = TransformsSimCLR(noise_type = "uniform")
img_T_pair = torch.stack([T_simCLR(img, flag_RdSm = False), T_simCLR(img, flag_RdSm = True)])

def get_color_distortion(s=0.5):
    color_jitter = torchvision.transforms.ColorJitter(0.8*s, 0.8*s, 0.8*s, 0.2*s)
    rnd_color_jitter = torchvision.transforms.RandomApply([color_jitter], p=0.8)
    rnd_gray = torchvision.transforms.RandomGrayscale(p=0.2)
    color_distort = torchvision.transforms.Compose([rnd_color_jitter, rnd_gray])
    return color_distort

class TransformsSimCLR:
    def __init__(self, noise_type, size = 32):
        self.train_transform = torchvision.transforms.Compose([
            torchvision.transforms.ToPILImage(),
            torchvision.transforms.RandomResizedCrop(size),
            torchvision.transforms.RandomHorizontalFlip(p=0.5),
            get_color_distortion(s=0.5),
            torchvision.transforms.ToTensor()])
        self.train_transform_smoothing = torchvision.transforms.Compose([
            torchvision.transforms.ToPILImage(),
            torchvision.transforms.RandomResizedCrop(size),
            torchvision.transforms.RandomHorizontalFlip(p=0.5),
            get_color_distortion(s=0.5),
            torchvision.transforms.ToTensor(),
            Perturb_In_Randmized_Smoothing(noise_type)
        ])
    def __call__(self, x, flag_RdSm = False):
        if not flag_RdSm:
            return self.train_transform(x)
        else:
            return self.train_transform_smoothing(x)

class Perturb_In_Randmized_Smoothing():
    def __init__(self, noise_type, noise_sd = 0.5):
        self.noise_type = noise_type
        self.noise_sd = noise_sd
    def __call__(self, img):
        if self.noise_type == "gaussian":
            img = torch.randn_like(img)*self.noise_sd + img
        elif self.noise_type == "uniform":
            img = (torch.randn_like(img) - 0.5)*2*self.noise_sd + img
        return img
```

B Performance on other SSL framework

We verified the performance of RUSH using BYOL [18] to replace SimCLR [17] in the pre-training stage. The training parameters follow the setting of Section 5.1.

Table 8: Performance using BYOL [18], in terms of standard accuracy, robust accuracy under $\ell_\infty=8/255$ PGD with ResNet-18 on CIFAR-10

Dataset	Methods	Acc.(%)		
		Standard	PGD	AA
CIFAR-10	RUSH \mathcal{I}_F^+ (ours)	84.7	71.3	-
	RUSH \mathcal{I}_F (ours)	82.9	66.8	-